Published in final edited form as:
Muscle Nerve. 2010 October ; 42(4): 522–529. doi:10.1002/mus.21724.

Mitochondrial redox potential during contraction in single intact muscle fibers

Luke P. Michaelson, MSN, **Guoli Shi, Ph.D.**, **Chris W. Ward, Ph.D.**, and **George G. Rodney, Ph.D.**
Organizational Systems and Adult Health, University of Maryland School of Nursing, 655 W. Lombard St., Baltimore, MD 21201

Abstract

Introduction—While the production of reactive oxygen species (ROS) during muscle contractile activity has been linked to both positive and negative adaptive responses, the sites for ROS generation within working muscle are not clearly defined.

Methods—We assessed cytosolic ROS production and mitochondrial redox potential with a targeted redox sensitive green fluorescent protein during repetitive field stimulation of single mature myofibers.

Results—Cytosolic ROS production increased by 94%, an effect that was abolished by pre-treatment with the reducing agent dithiothreitol. Mitochondrial redox potential was not altered during muscle contraction. In contrast, activity-dependent ROS production was ablated by an inhibitor of NADPH oxidase.

Discussion—We provide the first report on dynamic ROS production from mitochondria in single living myofibers and suggest that the mitochondria are not the major source of ROS during skeletal muscle contraction. Alternatively, our data support a role for NADPH oxidase-derived ROS during contractile activity.

Introduction

Skeletal muscle produces low levels of reactive oxygen species (ROS) that are required for normal contractile function, gene regulation and regulation of cellular signaling. High levels of ROS, however damage cellular components and result in contractile dysfunction and fatigue (for review see [1]). It has long been assumed that the mitochondria are the primary source of ROS formation in skeletal muscle cells and that the increased ROS generation that occurs during contractile activity is directly related to the increased oxygen consumption associated with increased mitochondrial activity. Reassessments of the rate of ROS production by mitochondria indicate that only 0.1% – 0.2% of the O_2 consumed is released as reactive oxygen [2, 3], about 10% less than originally thought. Thus, mitochondria may not be the primary source of ROS during contractile activity. Additional sites for ROS production within skeletal muscle include the NADPH oxidase $gp91^{phox}$, the cytosolic phospholipase A_2 and xanthine oxidase. The role each of these sources play in increased ROS production during contractile activity and pathology has been obscured by our inability to precisely detect ROS production in spatially-restricted regions of the cell. It is likely that

Corresponding Author: George G. Rodney, University of Maryland School of Nursing, 655 W. Lombard St., room 778, Baltimore, MD 21201, Voice: 410-706-3181, Fax: 410-706-0399, Rodney@son.umaryland.edu.

Author Disclosure Statement: No competing financial interests exist.

multiple sites of ROS generation are active under different situations and that the effects are relatively localized and important for distinct cellular functions.

The ROS-sensitive fluorescent indicator dichlorofluorescein (DCFH) has been used to assess ROS production in muscle homogenates [4, 5], isolated muscle strips/bundles and myotubes [6–12]. Although it is very useful in measuring rates of ROS production in the bulk cytosol, it does not allow for dynamic measurements of redox potential at discrete sub-cellular sites. Recently, redox-sensitive fluorescent proteins have been developed by inserting an artificial dithiol-disulfide pair into the structure of green fluorescent protein (GFP) [13]. These redox-sensitive GFPs (roGFP) allow for targeted expression (i.e. mitochondria and endoplasmic reticulum) of a reversible redox sensor within the cell [13, 14], providing a reliable method for investigations of local changes in redox potential within sub-cellular regions.

The aims of this study were to establish a reliable method to assess the production of ROS within single living skeletal muscle fibers and to dynamically evaluate the contribution of the mitochondria to intracellular ROS production during contractile activity. We measured cytosolic and mitochondrial ROS production during 15 minutes of repeated tetanic stimulation in single skeletal muscle fibers. Our findings indicate that the mitochondria do not significantly contribute to contraction-induced ROS production in skeletal muscle.

Materials and Methods

In-vivo electroporation

transfection of mitochondrially targeted redox sensitive GFPs (mito-roGFP, kind gift from S.J. Remington) into mouse flexor digitorum brevis (FDB) was as described by DiFranco et al [15] with some modifications. Male C57Bl wild-type mice (The Jackson Laboratory, Bar Harbor, MA) 6–8 weeks of age were anesthetized with isoflurane (2%) in accordance with National Institutes of Health guidelines and approved by the Institutional Animal Care and Use Committee of the University of Maryland Baltimore. Hyaluronidase (10μl of 1mg/ml) dissolved in sterile saline was injected subcutaneously into the right foot pad followed by 30–40 μg of rDNA in PBS 1 hour later. Two electrodes were placed subcutaneously at the proximal and distal tendons to deliver 20 pulses of 150 V, 20 ms in duration at a frequency of 1 Hz with a square pulse stimulator (S48; Grass Technologies, West Warwick, RI). Flexor digitorum brevis (FDB) muscle fibers were isolated 5 to 10 days later. Typically the right foot was electroporated, while the left foot served as a contra-lateral control.

Isolation of FDB fibers

Mice were deeply anesthetized by isofluorane (2%) inhalation and euthanized by thoracotomy/exsanguination. FDB muscles were surgically isolated and incubated in minimal essential media containing 0.1% gentamycin and 0.4% Collagenase A (Roche Applied Science, Indianapolis, IN) at 37°C for 1.5–2.0 hours. To release single fibers, FDB muscles were then triturated gently in media without collagenase. The fibers were then plated on ECM gel from Engelbreth-Holm-Swarm murine sarcoma (ECM) (Sigma, St. Louis, MO) coated 96 well culture dishes (Costar, Corning Incorporated Life Sciences, Lowell, MA) in serum-containing media (10%, Atlanta Biologicals) and incubated in 5% CO_2 at 37°C until used, typically 12–36 hrs later.

Loading of single FDB fibers with DCFH-DA

6-carboxy-2′,7′-dichlorodihydrofluorescein diacetate (DCFH-DA) (Invitrogen, Carlsbad, CA) was prepared in dimethyl sulfoxide (DMSO)/pluronic. Culture dishes containing isolated FDB fibers were washed with 4-(2-Hydroxyethyl)piperazine-1-ethanesulfonic acid

(HEPES) buffered Ringer's solution containing (in mM): 140 NaCl, 4.0 KCl, 1.0 $MgSO_4$, 5.0 $NaHCO_3$, 10.0 glucose, 10.0 HEPES, pH 7.3 and incubated with Ringer's solution containing DCFH-DA (10 μM) for 30 to 45 minutes at room temperature. The fibers were then washed with Ringer's solution and allowed to de-esterify the dye for 20 minutes prior to fluorescence microscopy. To prevent light induced oxidation of DCFH, all cell loading was performed in the dark.

Electrical stimulation of single FDB fibers

Isolated FDB myofibers were perfused with Ringer's solution for 1 minute to obtain a basal rate of DCFH oxidation. Subsequently, twitch (1.5 ms square pulse) and intermittent trains (0.25 Hz, 500 msec train duration) of tetanic stimulation (80 Hz) were delivered to isolated FDBs for 15 minutes via a custom-built perfusion/electrical stimulation chamber (Four Hour Day Foundation, Towson, MD). A perfusion controller (Valvebank 8 II; Automate Scientific) allowed rapid changing of perfusate during imaging. In some experiments FDB fibers underwent tetanic stimulation for 10 minutes, then the perfusate was changed to a Ringer's solution containing dithiothreitol (DTT) (10mM) for the remaining 5 minutes of the stimulation protocol. At the end of the 15 minute tetanic stimulation protocol, DCFH-loaded FDB fibers were exposed to Ringer's solution for 2 minutes followed by 500 μM H_2O_2 to obtain a maximal rate of DCFH oxidation for each fiber. Since the amount of DCFH loaded is variable from fiber to fiber we used the maximal rate of DCF fluorescence in the presence of 500 μm H_2O_2 to normalize the rate of DCF fluorescence for each fiber.

Fluorescence microscopy and image analysis

Dichlorofluorescin (DCF) and mito-roGFP fluorescence was monitored using a charge coupled device (CCD) Camera (CoolSnap HQ, Photometrics, Tucson, AZ) attached to an IX-50 (Olympus, Center Valley, PA) inverted microscope (40x H_2O objective, 1.2 NA). Mito-roGFP was excited at 400 nm (λ_1) and 480 nm (λ_2) while DCF was excited at 480 nm, and emission intensity for both probes was collected at 510 nm. Images were acquired at a rate of 0.33 Hz. Images were analyzed using IPLab 4.0 (Scanalytics, BD Biosciences, San Jose, CA). For Ca^{2+} transients, cells were loaded with mag-fluo-4 acetoxymethyl (AM) (Invitrogen) (10μM for 30 min at room temperature), and mag-fluo-4 fluorescence was recorded once every 2 minutes using an IonOptix fluorescence system (IonOptix, Milton, MA) attached to an Olympus IX-70 inverted (40x H_2O objective, 1.2 NA) microscope equipped with a Lambda DG4 excitation light source (Sutter Instrument, Novato, CA). For colocalization analysis mito-roGFP expressing FDBs were loaded with tetramethylrhodamine methyl ester (TMRM, 20 nM), and two-dimensional (X-Y) images were acquired sequentially on a BioRad Radiance fluorescent laser scanning confocal attached to an Olympus IX-70 inverted microscope (60x oil objective, 1.4 NA).

Calculation of redox potentials

The ratio of reduced over oxidized mito-roGFP was calculated for the entire FDB using equation 1 as previously reported [16].

$$\frac{R}{1-R}=\frac{F-F_{ox}}{F_{red}-F}\left(\frac{I_{ox}\lambda_2}{I_{red}\lambda_2}\right) \quad \text{and} \quad F=\frac{I_{\lambda 1}}{I_{\lambda 2}} \quad F_{ox}=\frac{I_{ox,\lambda 1}}{I_{ox,\lambda 2}} \quad F_{red}=\frac{I_{red,\lambda 1}}{I_{red,\lambda 2}} \tag{1}$$

Where I is the raw fluorescence intensity at 510nm upon excitation at either 400nm (λ1) or 480nm (λ2) excitation and I_{ox} and I_{red} are the raw fluorescence intensity under fully oxidizing (1mM H_2O_2) and fully reducing conditions (10mM DTT), respectively. The *in-*

vivo redox potential was calculated using the Nernst equation with $E^{\circ\prime}$roGFP=−291 mV as previously reported [14]:

$$E^{\circ'}\text{ambient}=E^{\circ'}\text{roGFP}-29.6\,\text{mV}\log(R/(1-R)) \quad (2)$$

Data Analysis

Data are reported as mean ± SEM, unless otherwise specified. Statistical analysis was performed in Sigma Stat (Systat Software Inc., San Jose, CA) with a significance level of $p < 0.05$. Colocalization analysis was performed in Volocity (Improvision).

Results

Contractile activity induces ROS production

When stimulated for 15 minutes with repeated 80 Hz tetani single FDB fibers showed a 31 ± 7% reduction in the twitch (pre-tetanic vs. post-tetanic, $n_{animals}=3$, $n_{fibers}=5$) and a 39 ± 7% reduction in tetanic (first tetanus vs. last tetanus, $n_{animals}=3$, $n_{fibers}=5$) Ca^{2+} transients, respectively (Fig. 1). To determine the rate of ROS production at a time in which the Ca^{2+} transient was decreased, we assessed DCF fluorescence within the FDB fibers during the last 3 minutes of tetanic stimulation (Fig 2). Figure 2a shows representative DCF fluorescence data (ΔF/F) over time. Fatiguing stimulation increased the rate of DCF fluorescence (dashed black line) compared to non-stimulated time matched controls (solid black line). DTT (10mM) decreased the oxidation of DCFH as can be seen by the decrease in the time-dependent change in DCF fluorescence (Fig. 2a, dashed grey line & Fig. 2b). Addition of 500 μM H_2O_2 resulted in a maximal rate of change in DCF fluorescence (Fig. 2a). On average the rate of change in DCF fluorescence in the presence of 500μM H_2O_2 was not different between non-stimulated time controls and stimulated FDB fibers (9.19 ± 1.93 vs. 6.82 ± 1.79, respectively, P=0.38); higher H_2O_2 concentrations did not significantly increase the rate of DCF fluorescence (data not shown). To control for variable loading of DCFH-DA into the muscle fibers we normalized the rate of change in DCF fluorescence to the maximum rate obtained in the presence of 500 μM H_2O_2 on a fiber by fiber basis. Tetanic stimulation significantly increased (94%) the normalized rate of DCF fluorescence compared to the basal period ($1.09\times10^{-2} \pm 3.84\times10^{-3}$ vs. $5.61\times10^{-3} \pm 1.57\times10^{-3}$, respectively, $n_{animals}=4$, $n_{fibers}=11$, Fig 2b). The normalized rate of DCF fluorescence in non-stimulated time-matched control fibers ($5.71\times10^{-3} \pm 9.11\times10^{-4}$, $n_{animals}=5$, $n_{fibers}=10$) was not different than the pre-stimulated basal period (P=0.96), indicating that the increase in DCF fluorescence with contractile activity is not simply due to photo-oxidation of DCFH but also to ROS production from the single muscle fiber. Addition of DTT (10 mM) after 10 minutes of tetanic stimulation significantly decreased the normalized rate of DCF fluorescence ($1.56\times10^{-3} \pm 1.69\times10^{-3}$, $n_{animals}=4$, $n_{fibers}=10$). In the absence of tetanic stimulation, DTT decreased the normalized rate of DCF fluorescence during the last 3 minutes compared to fibers not exposed to DTT, but this did not reach statistical significance ($1.56\times10^{-3} \pm 1.69\times10^{-3}$ vs. $5.71\times10^{-3} \pm 9.10\times10^{-4}$, respectively, ANOVA P=0.065). Taken together, these data show that contractile activity increased ROS production in single adult skeletal muscle fibers.

Mitochondria do not mediate increased ROS formation with contractile activity

To determine the contribution of the mitochondria to contractile activity-induced ROS production we expressed a mitochondrially targeted GFP based redox sensor (mito-roGFP) in FDBs. Figure 3A shows that *in-vivo* electroporation of FDB muscle resulted in fiber fluorescence upon 488 nm excitation. Co-labeling of single FDB fibers that express mito-roGFP with TMRM (20 nM) shows targeting of the redox sensor to the mitochondria (Fig.

3B) Colocalization analysis confirms that mito-roGFP colocalizes with the mitochondrial marker TMRM (m_x=0.890, m_y=0.916). Using equation 1 we calculated the mitochondrial redox potential for a large region of interest (>70%) of FDB fibers under basal non-stimulated conditions and during the last 3 minutes of the 15 minute contractile activity (Fig. 3C). There was no difference in the mitochondrial redox potential at the end of the15 minutes of electrical stimulation compared to the basal state (−293 ± 4 mV and −294 ± 3 mV respectively, $n_{animals}$=4 n_{fibers}=17). Application of exogenous H_2O_2 (1 mM) and DTT (10 mM) to obtain fluorescence under maximum oxidizing (F_{ox}) and reducing (F_{red}) conditions respectively, resulted in a 2 to 3-fold change in the 400/480 ratio, showing that mito-roGFP responds to oxidizing and reducing agents (data not shown). Thus, under the stimulation protocol used in these experiments the mitochondria did not contribute significantly to the increased ROS production.

NADPH oxidase plays a role in ROS production with contractile activity

To further investigate the source of increased ROS production with contractile activity we assessed the role of plasma membrane-bound NADPH oxidase. Isolated fibers were pre-incubated with the NADPH oxidase inhibitors diphenyleneiodonium chloride (DPI, 10 μM) or apocynin (25 μM) for 30 minutes prior to the contractile period. In DPI treated myofibers ($n_{animals=}$3, $n_{fibers=}$13) the basal rate of DCFH oxidation was significantly reduced (77%) compared to non-DPI treated controls ($1.38\times10^{-3} \pm 7.60\times10^{-4}$ vs. $6.12\times10^{-3} \pm 1.89\times10^{-3}$ respectively, Fig. 4), suggesting that a portion of basal ROS production in skeletal muscle is via NADPH oxidase. DPI also significantly reduced (95%) the normalized rate of DCFH oxidation observed with increased contractile activity ($5.00\times10^{-3} \pm 2.65\times10^{-4}$, Fig. 4). Fibers treated with apocynin were consistently found to not survive the electrical stimulation protocol. Apocynin has been shown to stimulate ROS production in non-phagocytic cells [17], therefore we assessed the effect of apocynin on DCFH oxidation. We found that apocynin resulted in a 47% increase in DCFH oxidation during the 30 minute incubation period. These data demonstrate that skeletal muscle NADPH oxidase generates ROS under basal conditions and increases ROS production in an activity-dependent manner.

Discussion

Although it is clear that skeletal muscle produces ROS under resting conditions and that exercise increases ROS production, the source(s) of these oxidants have remained unclear. In these studies we utilized a novel dynamic redox sensor targeted to the mitochondria to address mitochondrial ROS production during contractile activity in intact, single living skeletal muscle fibers. We demonstrated that the plasma membrane-bound NADPH oxidase plays a crucial role in exercise-induced ROS production. Our data provide little support for involvement of mitochondrial ROS production with increased contractile activity.

Increased contractile activity increases ROS production

Previous studies that assessed the production of ROS in contracting skeletal muscle have been from either homogenized tissue subsequent to a bout of exercise or from whole muscle bundles [4, 5, 8–11]. Disruption of tissues during homogenization or other cell types in whole bundle experiments may give rise to artifactual changes in ROS production and makes it difficult to assess what fraction of the increased ROS comes directly from skeletal muscle cells. More recently, ROS production has been assessed in intact living skeletal muscle fibers [18, 19], however, the site of ROS production remains uncertain. Here we have taken advantage of our well characterized single adult mouse FDB myofiber preparation [20, 21] to assess the site of ROS production in intact myofibers in response to increased contractile activity.

Fifteen minutes of repeated tetanic stimulation of single FDB muscle fibers resulted in a 31% decrease in the peak twitch Ca^{2+} transient and a 39% decrease in the peak tetanic Ca^{2+} transient (Fig. 1). Although we did not measure force in our experiments, the decrease in peak $[Ca^{2+}]_i$ transients observed with our electrical stimulation paradigm is consistent with the late phase of muscle fatigue [22]. We also found an increase in the rate of ROS production by 91% compared with non-stimulated muscle fibers (Fig. 2b). These results are qualitatively similar to those of Jackson and colleagues [23] who reported an ~58% increase in DCF fluorescence with electrical stimulation in single intact FDB fibers

Oxidation of DCFH can occur by a variety of reactive oxygen and nitrogen species, thus we cannot ascertain which species is increased with electrical stimulation. Since our preparation contains only skeletal muscle fibers, the increase in DCFH oxidation observed is due to reactive species produced by the muscle fiber and not other cell types. Our data support the hypothesis that skeletal muscle fibers produce ROS and that ROS production is increased with muscle contraction.

Source of ROS in contracting skeletal muscle

The source(s) of oxidant production from skeletal muscle during exercise remains undetermined. Potential sources of ROS include mitochondria, membrane-bound NADPH oxidase, xanthine oxidase, cyclooxygenase, P-450-dependent monooxygenase, and lipoxygenase. It has long been assumed that, as oxygen consumption increases with exercise, the amount of ROS produced by the mitochondria also increases. This implies that the mitochondria are the major source of ROS in exercising skeletal muscle. Studies supporting this concept have come from *in-vitro* studies of isolated mitochondria [24, 25] under non-physiological conditions. More recently superoxide production, as assessed by MitoSOX Red fluorescence, in FDB fibers during repeated tetanic stimulation was found not to increase [18]. Thus, the contribution of mitochondria-derived ROS to the changes in cellular redox status of skeletal muscle during contractile activity remains unclear.

In these studies we used a novel reversible redox-sensitive GFP construct targeted to the mitochondria (mito-roGFP) to assess the contribution of the mitochondria to increased ROS production observed with electrical stimulation in single intact skeletal muscle fibers. Use of mito-roGFP offers several advantages for assessing mitochondrial ROS production. First, the indicator is ratiometric by excitation, reducing measurement errors due to changes in indicator concentration, variable cell thickness, photobleaching and photooxidation. Second, the indicator is responsive to both oxidation and reduction. This dynamic response allows for the redox potential of the probe environment to be quantitatively determined. We found that a level of contractile activity that decreases $[Ca^{2+}]_i$ transients and increases cytosolic DCFH oxidation did not alter the redox state of the mitochondria when compared to non-stimulated muscle fibers (Fig. 3), arguing against the mitochondria as a major source of ROS production with this contraction protocol.

We were surprised to find that the tetanic stimulation protocol used in these studies did not result in changes in the mitochondrial redox potential. As discussed above, Aydin et al did not find a change in MitoSOX Red fluorescence upon tetanic stimuation of single FDB fibers [18], suggesting that superoxide production was not increased with increased contractile activity. Furthermore, it has been suggested that during aerobic contractile activity skeletal muscle mitochondria are in state III respiration [26, 27], which limits ROS production. Taken together, these data argue against major formation of ROS within mitochondria during increased contractile activity. This is not to say that mitochondrial redox potential will remain constant under different conditions. In our studies we assessed the mitochondrial redox potential of fast-twitch muscle fibers contracting under no load at 22 °C. Muscle temperature has been shown to effect ROS-dependent fatigue of skeletal muscle [28], with an

enhancement at 37 °C compared to 22 °C. In addition, the redox potential of the mitochondria is likely to depend on cellular energy usage and show changes with increased work-load on the muscle (e.g. eccentric contractions) or in fibers with increased mitochondrial content (e.g. slow-twitch fibers). We are currently investigating the contribution of these factors to mitochondrial redox potential in contracting skeletal muscle.

NADPH oxidase (NOX) is a family of multiprotein enzymes that was first characterized in phagocytic cells. The active oxidase is made up of several protein components, including two membrane proteins, gp91^{phox} and p22^{phox} (also known as cytochrome b_{558}), three cytosolic proteins, p47^{phox}, p67^{phox}, and the small GTP-binding protein Rac. Upon stimulation, the cytosolic proteins translocate to the membrane to form a complex with cytochrome b_{558}, which results in enzymatic activation and production of $O_2^{\bullet-}$ (reviewed in [29, 30]). In recent years, NOX enzymes have been localized to the plasma membrane and transverse tubules in skeletal muscle [31, 32] and have been implicated in ROS formation with depolarization [33], osmotic stress [34], as well as the exercise pressor reflex [35]. Here we found that DPI reduced the basal rate of DCFH oxidation and nearly abolished the rate of contraction-induced DCFH oxidation (Fig. 4). DPI inhibits other flavoenzymes and therefore is not a highly specific inhibitor of NOX.

Inhibition of mitochondrial NADH-ubiquinone oxidoreductase (mitochondrial Complex I) by DPI was reported only during reverse electron transport, without affecting $O_2^{\bullet-}$ generation during forward electron transport [36]. Thus, in our studies the reduction in DCFH oxidation by DPI is not likely through complex I inhibition. Along with DPI, apocynin has been used extensively to implicate NOX enzymes in ROS generation in many cell types. We found that FDB fibers pre-incubated with apocynin did not survive the electrical stimulation. Apocynin increased the rate of DCFH oxidation (47%) during the pre-incubation period and in the absence of electrical stimulation. Apocynin has previously been shown to increase ROS formation in non-phagocytic cells [17], which we now show in adult skeletal muscle fibers. We hypothesize that the apocynin-induced ROS formation results in oxidation of key components necessary for cell survival. Although we cannot completely rule out other sources of ROS, our results suggest that NADPH oxidase in skeletal muscle plays an important role in ROS production during contractile activity.

In phagocytes NADPH oxidase is oriented to produce extracellular $O_2^{\bullet-}$ [37]. In non-phagocytic cells there is some controversy as to the orientation of the enzyme and whether $O_2^{\bullet-}$ is produced intracellularly or extracellulary (for review see [38]). Skeletal muscle has been shown to release $O_2^{\bullet-}$ to the extracellular space [11, 39]. Whether skeletal muscle NADPH oxidase is the source of this $O_2^{\bullet-}$ is unclear, since in those studies whole muscle bundles were used. The released $O_2^{\bullet-}$ could be from vascular smooth muscle NADPH oxidase. In our studies we observed a reduction in the rate of cytosolic DCFH oxidation upon inhibition of NADPH oxidase with DPI. We cannot determine whether oxidation of DCFH is due to $O_2^{\bullet-}$ released into the intracellular space or alternatively $O_2^{\bullet-}$ released extracellulary where it can spontaneously dismute to H_2O_2. In the second scenario H_2O_2 would have to cross the plasma membrane in order to oxidize DCFH. Since we are using single isolated muscle fibers we can conclude that skeletal muscle-specific NADPH oxidase is responsible for DCFH oxidation. Taken together, there is a growing body of evidence to suggest that NADPH oxidase plays a key role in skeletal muscle ROS production. Whether NADPH oxidase is involved in additional ROS signaling pathways such as stretch-activated ROS-stimulated glucose uptake [40] remains to be elucidated.

Summary

Our data are the first to assess the redox potential of skeletal muscle mitochondria in single intact living fibers and support the conclusion that mitochondria do not significantly

contribute to ROS production under the contractile paradigm reported here. Our data support a role for the membrane bound non-phagocytic NADPH oxidase in contraction-induced ROS production. Our ability to detect sub-cellular production of ROS in living skeletal muscle fibers will shed new light on the role of ROS in cell signaling processes, setting the stage for development of targeted antioxidant therapies to combat the destructive effects of free radicals in muscle and cardiovascular diseases.

Supplementary Material

Refer to Web version on PubMed Central for supplementary material.

Acknowledgments

The authors thank Dr. S.J. Remington (University of Oregon) for the generous gift of cDNA coding for mitochondrial targeted roGFP. This work was supported by an Individual National Research Award (NINR - F32-NR011245) to L.P.M., an R-03 (NIAMS - AR053318) to C.W.W., and a Mentored Research Scientist Development Award (NIAMS - K01 AR-051519) to G.G.R.

List of Abbreviations

AM	acetoxymethyl
CCD	charge coupled device
DCF	dichlorofluorescin
DCFH	dichlorodihydrofluorescein
DCFH-DA	dichlorodihydrofluorescein diacetate
DMSO	dimethyl sulfoxide
DPI	diphenyleneiodonium chloride
DTT	dithiothreitol
ECM	ECM gel from Engelbreth-Holm-Swarm murine sarcoma
FDB	flexor digitorum brevis
GFP	green fluorescent protein
HEPES	4-(2-Hydroxyethyl)piperazine-1-ethanesulfonic acid
H_2O_2	hydrogen peroxide
mito-roGFP	mitochondrial redox sensitive GFP
ROS	reactive oxygen species

References

1. Powers SK, Jackson MJ. Exercise-Induced Oxidative Stress: Cellular Mechanisms and Impact on Muscle Force Production. Phys Rev. 2008; 88:1243–1276.
2. St-Pierre J, Buckingham JA, Roebuck SJ, Brand MD. Topology of superoxide production from different sites in the mitochondrial electron transport chain. J Biol Chem. 2002; 277:44784–44790. [PubMed: 12237311]
3. Tahara EB, Navarete FD, Kowaltowski AJ. Tissue-, substrate-, and site-specific characteristics of mitochondrial reactive oxygen species generation. Free Radic Biol Med. 2009; 46:1283–1297. [PubMed: 19245829]
4. Bejma J, Ji LL. Aging and acute exercise enhance free radical generation in rat skeletal muscle. J Appl Physiol. 1999; 87:465–470. [PubMed: 10409609]

5. Davies KJ, Quintanilha AT, Brooks GA, Packer L. Free radicals and tissue damage produced by exercise. Biochem Biophys Res Commun. 1982; 107:1198–1205. [PubMed: 6291524]
6. Arbogast S, Reid MB. Oxidant activity in skeletal muscle fibers is influenced by temperature, CO2 level, and muscle-derived nitric oxide. Am J Physiol Regul Integr Comp Physiol. 2004; 287:R698–R705. [PubMed: 15178539]
7. Nethery D, Stofan D, Callahan L, DiMarco A, Supinski G. Formation of reactive oxygen species by the contracting diaphragm is PLA(2) dependent. J Appl Physiol. 1999; 87:792–800. [PubMed: 10444641]
8. Reid MB, Haack KE, Franchek KM, Valberg PA, Kobzik L, West MS. Reactive oxygen in skeletal muscle. I. Intracellular oxidant kinetics and fatigue in vitro. J Appl Physiol. 1992; 73:1797–1804. [PubMed: 1474054]
9. Kolbeck RC, She ZW, Callahan LA, Nosek TM. Increased superoxide production during fatigue in the perfused rat diaphragm. Am J Respir Crit Care Med. 1997; 156:140–145. [PubMed: 9230738]
10. Jackson MJ, Edwards RH, Symons MC. Electron spin resonance studies of intact mammalian skeletal muscle. Biochim Biophys Acta. 1985; 847:185–190. [PubMed: 2998478]
11. Reid MB, Shoji T, Moody MR, Entman ML. Reactive oxygen in skeletal muscle. II. Extracellular release of free radicals. J Appl Physiol. 1992; 73:1805–1809. [PubMed: 1335453]
12. Pattwell DM, McArdle A, Morgan JE, Patridge TA, Jackson MJ. Release of reactive oxygen and nitrogen species from contracting skeletal muscle cells. Free Radic Biol Med. 2004; 37:1064–1072. [PubMed: 15336322]
13. Hanson GT, Aggeler R, Oglesbee D, Cannon M, Capaldi RA, Tsien RY, Remington SJ. Investigating Mitochondrial Redox Potential with Redox-sensitive Green Fluorescent Protein Indicators. J Biol Chem. 2004; 279:13044–13053. [PubMed: 14722062]
14. Dooley CT, Dore TM, Hanson GT, Jackson WC, Remington SJ, Tsien RY. Imaging Dynamic Redox Changes in Mammalian Cells with Green Fluorescent Protein Indicators. J Biol Chem. 2004; 279:22284–22293. [PubMed: 14985369]
15. DiFranco M, Neco P, Capote J, Meera P, Vergara JL. Quantitative evaluation of mammalian skeletal muscle as a heterologous protein expression system. Protein Expression and Purification. 2006; 47:281–288. [PubMed: 16325422]
16. Lohman JR, Remington SJ. Development of a Family of Redox-Sensitive Green Fluorescent Protein Indicators for Use in Relatively Oxidizing Subcellular Environments. Biochemistry. 2008; 47:8678–8688. [PubMed: 18652491]
17. Vejrazka M, MØcek R, StØpek S. Apocynin inhibits NADPH oxidase in phagocytes but stimulates ROS production in non-phagocytic cells. Biochimica et Biophysica Acta (BBA) - General Subjects. 2005; 1722:143–147.
18. Aydin J, Andersson DC, Hanninen SL, Wredenberg A, Tavi P, Park CB, Larsson NG, Bruton JD, Westerblad H. Increased mitochondrial Ca^{2+} and decreased sarcoplasmic reticulum Ca^{2+} in mitochondrial myopathy. Hum Mol Genet. 2009; 18:278–288. [PubMed: 18945718]
19. Bruton JD, Place N, Yamada T, Silva JP, Andrade FH, Dahlstedt AJ, Zhang SJ, Katz A, Larsson NGr, Westerblad H. Reactive oxygen species and fatigue-induced prolonged low-frequency force depression in skeletal muscle fibres of rats, mice and SOD2 overexpressing mice. J Physiol (Lond). 2008; 586:175–184. [PubMed: 18006575]
20. Brown L, Rodney G, Hernandez-Ochoa E, Ward C, Schneider MF. Calcium sparks and T-tubule reorganization in dedifferentiating adult mouse skeletal muscle fibers. Am J Physiol Cell Physiol. 2006; 292:C1156–C1166. [PubMed: 17065203]
21. Rodney GG. Calmodulin in Adult Mammalian Skeletal Muscle: Localization and Effect on Sarcoplasmic Reticulum Ca^{2+} Release. Am J Physiol Cell Physiol. 2008; 294:C1288–C1297. [PubMed: 18322139]
22. Allen DG, Lamb GD, Westerblad H. Skeletal Muscle Fatigue: Cellular Mechanisms. Phys Rev. 2008; 88:287–332.
23. Palomero J, Pye D, Kabayo T, Spiller DG, Jackson MJ. In Situ Detection and Measurement of Intracellular Reactive Oxygen Species in Single Isolated Mature Skeletal Muscle Fibers by Real Time Fluorescence Microscopy. Antioxid Redox Signal. 2008; 10:1463–1474. [PubMed: 18407749]

24. Venditti P, Bari A, Di SL, Di MS. Role of mitochondria in exercise-induced oxidative stress in skeletal muscle from hyperthyroid rats. Arch Biochem Biophys. 2007; 463:12–18. [PubMed: 17395147]
25. Radák Z, Sasvári M, Nyakas C, Taylor AW, Ohno H, Nakamoto H, Goto S. Regular Training Modulates the Accumulation of Reactive Carbonyl Derivatives in Mitochondrial and Cytosolic Fractions of Rat Skeletal Muscle. Archives of Biochemistry and Biophysics. 2000; 383:114–118. [PubMed: 11097183]
26. Di MS, Venditti P. Mitochondria in exercise-induced oxidative stress. Biol Signals Recept. 2001; 10:125–140. [PubMed: 11223645]
27. Kozlov AV, Szalay L, Umar F, Kropik K, Staniek K, Niedermuller H, Bahrami S, Nohl H. Skeletal muscles, heart, and lung are the main sources of oxygen radicals in old rats. Biochim Biophys Acta. 2005; 1740:382–389. [PubMed: 15949706]
28. Moopanar TR, Allen DG. Reactive oxygen species reduce myofibrillar Ca^{2+}-sensitivity in fatiguing mouse skeletal muscle at 37 °C. J Physiol. 2005; 564:189–199. [PubMed: 15718257]
29. Bedard K, Krause KH. The NOX Family of ROS-Generating NADPH Oxidases: Physiology and Pathophysiology. Phys Rev. 2007; 87:245–313.
30. Dworakowski R, Anilkumar N, Zhang M, Shah AM. Redox signalling involving NADPH oxidase-derived reactive oxygen species. Biochem Soc Trans. 2006; 34:960–964. [PubMed: 17052237]
31. JAVESGHANI DANE, MAGDER SA, BARREIRO ESTH, QUINN MT, HUSSAIN SNA. Molecular Characterization of a Superoxide-Generating NAD(P)H Oxidase in the Ventilatory Muscles. Am J Respir Crit Care Med. 2002; 165:412–418. [PubMed: 11818330]
32. Hidalgo C, Sanchez G, Barrientos G, Aracena-Parks P. A transverse tubule NOX activity stimulates calcium release from isolated triads via RYR1 S-Glutathionylation. J Biol Chem. 2006; 281:26473–26482. [PubMed: 16762927]
33. Espinosa A, Leiva A, Pena M, Muller M, Debandi A, Hidalgo C, Carrasco MA, Jaimovich E. Myotube depolarization generates reactive oxygen species through NAD(P)H oxidase; ROS-elicited Ca^{2+} stimulates ERK, CREB, early genes. J Cell Physiol. 2006; 209:379–388. [PubMed: 16897752]
34. Martins AS, Shkryl VM, Nowycky MC, Shirokova N. Reactive oxygen species contribute to Ca^{2+} signals produced by osmotic stress in mouse skeletal muscle fibres. J Physiol (Lond). 2008; 586:197–210. [PubMed: 17974587]
35. Wang HJ, Pan YX, Wang WZ, Zucker IH, Wang W. NADPH Oxidase-Derived Reactive Oxygen Species in Skeletal Muscle Modulates the Exercise Pressor Reflex. J Appl Physiol. 2009; 107:450–459. [PubMed: 19498097]
36. Majander A, Finel M, Wikstrom M. Diphenyleneiodonium inhibits reduction of iron-sulfur clusters in the mitochondrial NADH-ubiquinone oxidoreductase (Complex I). J Biol Chem. 1994; 269:21037–21042. [PubMed: 8063722]
37. Lambeth JD. NOX enzymes and the biology of reactive oxygen. Nat Rev Immunol. 2004; 4:181–189. [PubMed: 15039755]
38. Griendling KK, Sorescu D, Ushio-Fukai M. NAD(P)H oxidase: role in cardiovascular biology and disease. Circ Res. 2000; 86:494–501. [PubMed: 10720409]
39. Zuo L, Christofi FL, Wright VP, Liu CY, Merola AJ, Berliner LJ, Clanton TL. Intra-and extracellular measurement of reactive oxygen species produced during heat stress in diaphragm muscle. Am J Physiol Cell Physiol. 2000; 279:C1058–C1066. [PubMed: 11003586]
40. Chambers MA, Moylan JS, Smith JD, Goodyear LJ, Reid MB. Stretch-stimulated glucose uptake in skeletal muscle is mediated by reactive oxygen species and p38 MAP-Kinase. J Physiol (Lond). 2009; 587:3363–3373. [PubMed: 19403598]

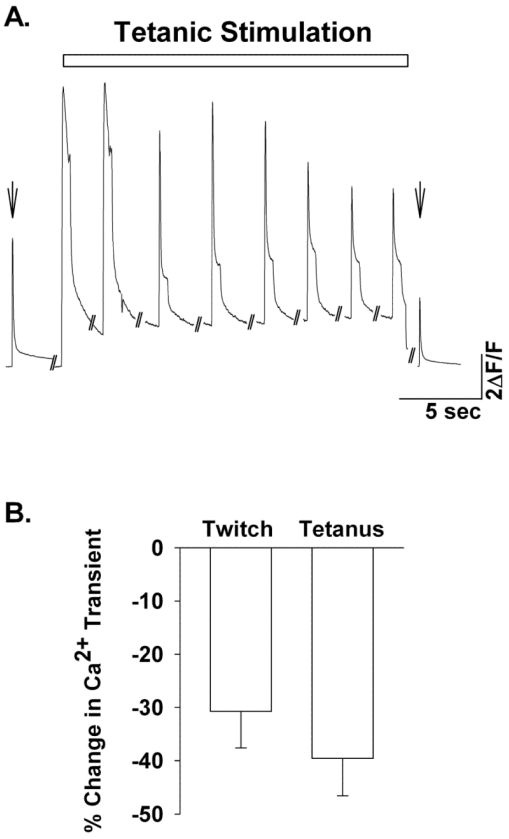

Figure 1.

Increased contractile activity reduces cytosolic Ca^{2+} transients. (A). Representative Ca^{2+} transients from single FDB myofibers. Shown are pre- and post-twitch $[Ca^{2+}]_i$ transients (arrow) and tetanic $[Ca^{2+}]_i$ transients recorded every 2 minutes during the 15 minute stimulation period. (B). Average decrement in twitch and titanic $[Ca^{2+}]_i$ transients in single isolated FDB fibers (n=6). Post-tetanic twitch Ca^{2+} transients were decreased (31%) when compared to pre-tetanic twitch Ca^{2+} transients. Tetanic Ca^{2+} transients measured as the peak of the Mag-fluo4 signal during the first and last tetani also decreased over the duration of the stimulation protocol (39%).

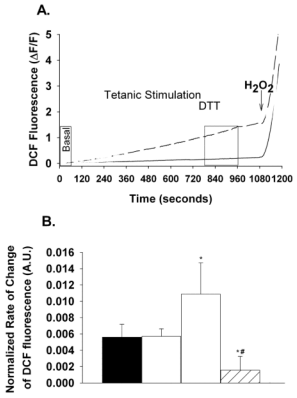

Figure 2.

Electrical stimulation increases the rate of DCF fluorescence in single adult FDB muscle fibers. (A). Representative data (ΔF/F) from single FDB fibers showing the temporal change in DCF fluorescence acquired once every 3 seconds (F is the fluorescence taken over the first 15 seconds of recording) in non-stimulated (solid line) and electrically stimulated (dashed line) muscle fibers. Perfusion of DTT (10mM, grey lines) 10 minutes after the start of the tetanic stimulation for the remaining 5 minutes blunted the increase in DCF fluorescence. Application of H_2O_2 (500 μM, arrow) was used to obtain a maximum rate of DCF oxidation for each fiber. (B). Average rate of change in DCF fluorescence prior to stimulation and during the last 3 minutes of stimulation (boxed areas in A) was normalized to the maximum rate observed in the presence of 500 μM H_2O_2. On average, tetanic stimulation significantly increased the normalized rate of DCF fluorescence (open bar) by 94% compared to paired pre-stimulated values (black bar, paired t-test) and 91% compared to non-stimulated time controls (grey bar). DTT (10 mM, grey hatched bar) prevented the tetanic stimulation induced increase in DCF fluorescence (ANOVA). $P<0.05$ *vs. pre-stimulated and non-stimulated, # vs. stimulated.

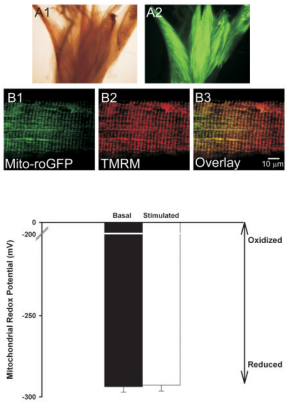

Figure 3.

Mitochondrial redox potential does not change with electrical stimulation. Wide field light (A1) and fluorescent (A2) images of FDB muscle bundles electroporated with mito-roGFP. Confocal image of a single FDB muscle fiber showing expression of mito-roGFP (B1). Staining with the mitochondrial indicator TMRM (B2) shows that expression of roGFP is localized to the mitochondria with co-localization coefficients m_x=0.890 and m_y=0.916 (B3, overlay). Panel C shows the average redox potential (n=17) under basal conditions and during the last 3 minutes of the 15 minute electrical stimulation period. No significant difference was found in the mitochondrial redox potential with electrical stimulation.

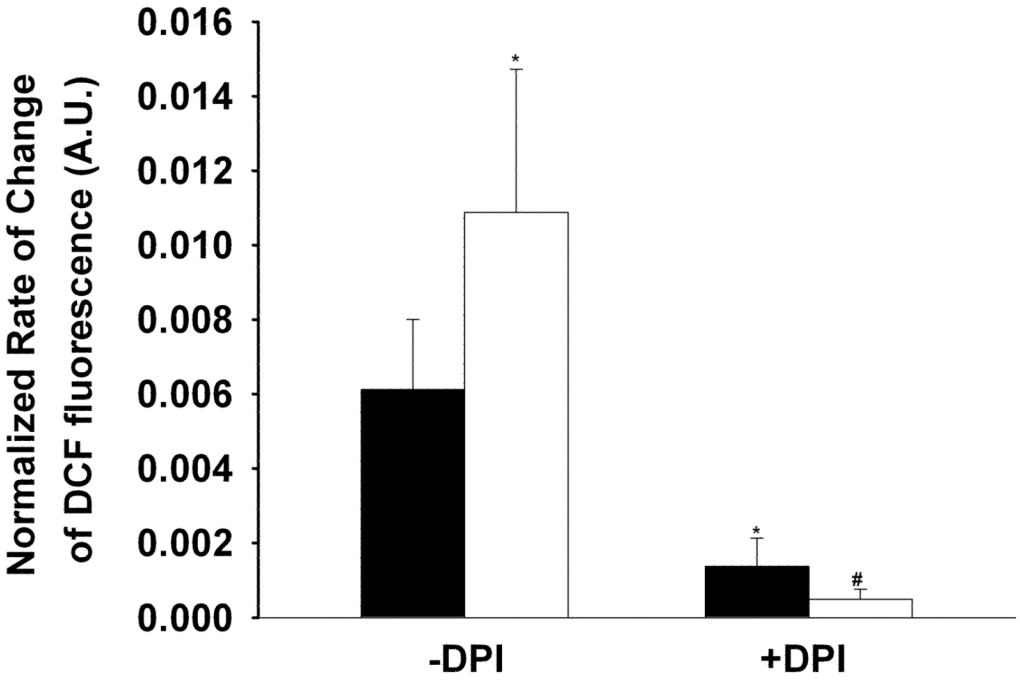

Figure 4.

Inhibition of NADPH oxidase prevents ROS formation. Bars show the rate of change in DCF fluorescence before stimulation (black bars) and during the last 3 minutes of tetanic stimulation (open bars) normalized to the maximum rate of change in DCF fluorescence in the presence of H_2O_2 (500 μM). Pre-incubaiton of FDB fibers ($n_{animals}$=3, n_{fibers}=13) with DPI (10 μM) reduces the basal rate of ROS formation compared to that observed in the absence of DPI (ANOVA, $P<0.05$) and prevents the tetanic stimulation induced ROS formation (ANOVA, $P<0.001$). No difference was observed in the DPI treated myofibers between basal and stimulated conditions (paired t-test). Data in the absence of DPI were taken from that shown in Figure 2.

*significantly different from baseline –DPI, #significantly different from tetanic stimulation – DPI.